Dynamic Modeling of Unsteady Bulging in Continuous Casting of Steel

Zhelin Chen, Hamed Olia, Bryan Petrus, Madeline Rembold, Joseph Bentsman and Brian G. Thomas

Abstract Mold level fluctuations caused by unsteady bulging of the solidifying shell affect the quality of the steel and stable operation of the continuous steel casting process. A dynamic bulging model, which captures the behavior of the 2-D longitudinal domain through interpolation of multiple 1-D moving slices, is used to calculate the transient bulging profile, volume changes caused by unsteady bulging, and the accompanying level fluctuations in the mold. The liquid steel flow rate through the SEN into the tundish is calculated with a stopper-position-based model. These two models are combined to investigate mold level fluctuations in a thin-slab caster under real casting conditions. The model is verified by comparing the simulation results with transient measurements in a commercial thin-slab caster.

Keywords Continuous casting · Unsteady bulging · Mold level fluctuation Stopper rod flow model · Dynamic bulging model

Introduction

In the continuous casting of steel, bulging is an important phenomenon where the internal ferrostatic pressure, partially restrained by the support rolls, causes the partially solidified shell to bulge outward between each pair of rolls. Bulging is directly responsible for internal cracks, centerline segregation, and permanent slab-width variations [1–3]. It also increases roll forces and roll wear. In addition, time variations of the bulged shape may cause volume changes of the molten steel contained within the solidifying shell in the strand, leading to mold level fluctuations. Such fluc-

Z. Chen · J. Bentsman
University of Illinois at Urbana-Champaign, 1206 W Green St, Urbana, IL 61801, USA

H. Olia · B. G. Thomas (✉)
Colorado School of Mines, 1610 Illinois St, Golden, CO 80401, USA
e-mail: bgthomas@mines.edu

B. Petrus · M. Rembold
Nucor Steel Decatur, 4301 Iverson Blvd, Trinity, AL 35673, USA

G. Lambotte et al. (eds.), *Materials Processing Fundamentals 2019*, The Minerals, Metals & Materials Series, https://doi.org/10.1007/978-3-030-05728-2_3

tuations may correspond to the time period between certain roll pitches, or certain roll diameters in different zones of the caster [3, 4].

It is well known that excessive mold level fluctuations lead to strand surface cracks and even breakouts. Mold level control has been studied for many years [5, 6] to minimize these problems. However, the mold level control system has difficulty recognizing and responding to dynamic bulging and cannot prevent it. Other methods, such as increasing the spray cooling in the secondary cooling region to decrease the surface temperature and thicken the shell, and adoption of non-uniform roll pitch have been proposed to reduce dynamic bulging problems [3, 7].

Previous work to study bulging has focused mainly on steady bulging, using Finite Element Analysis (FEM) [1, 8, 9]. A few recent studies have measured unsteady bulging in the casting machine using position detectors between rolls [3, 4, 7]. Such detectors are useful for model validation but are very difficult for everyday online use, especially for thin-slab casters, and have never been used to help mold level control systems.

To the authors' best knowledge, this work is the first attempt to develop a dynamic bulging model that is calculated fast enough for implementation into real-time online control systems and validated with plant measurements. A dynamic model, ConOffline [10–13], which captures the behavior of the 2-D longitudinal domain through interpolation of multiple 1-D moving slices, is used to calculate the bulging amplitudes. A new dynamic volume model then calculates the volume change induced by dynamic bulging and stopper rod movement. This model is verified with plant measurements and applied to gain new insight into the dynamic bulging phenomenon.

Model Description

Heat Transfer and Steady Bulging Model

First, shell thickness and temperature distribution in the continuous cast strand were predicted using ConOffline, an off-line version of the ConOnline model [10], which has been validated and used in many previous studies [11–14]. ConOffline solves the transient heat conduction equation within many transverse slices through the center of the strand using an explicit finite-difference method in a Lagrangian reference frame, which moves with the steel in the z-direction at the casting speed v_c:

$$\rho c_p^* \frac{\partial T}{\partial t} = \frac{\partial}{\partial x}\left(k \frac{\partial T}{\partial x}\right) \tag{1}$$

where x is the thickness direction, T is temperature, and temperature-dependent properties are density ρ, thermal conductivity k, and effective specific heat c_p^* which includes the latent heat, L_f and f_s is the solid fraction:

$$c_p^* = c_p + L_f \frac{df_s}{dT} \tag{2}$$

The caster and casting conditions simulated in this work were based on the thin-slab (90 mm) caster at Nucor Steel, Decatur. Average heat flux in the mold was based on an empirical correlation from Duvvuri [15]:

$$Q_m\left[M\,W/m^2\right] = 1.197(v_c)^{0.544} \tag{3}$$

Heat flux from the spray water in the secondary cooling zones was based on Nozaki's empirical correlation [16]:

$$h_{spray} = 0.3925 \times Q_{water}^{0.55} \times \left(1 - 0.0075 \times T_{spray}\right) \tag{4}$$

where $Q_{water}\left(L/m^2\right)$ is water flux in the spray zone and T_{spray} is the water temperature. Heat transfer in secondary cooling is a subject of ongoing research, and other relations are available and used at different casters.

ConOffline simulates $N = 200$ slices simultaneously; each slice starts at the meniscus at a different time to achieve a fixed z-direction spacing between slices. Then, the maximum bulging amplitude, $\delta_{\max}$, within each roll pitch is found from the following equation based on fitting many FEM simulations, proposed by Yu [8], knowing the local strand surface temperature, shell thickness, roll pitch, and ferrostatic pressure calculated using $P = \rho g h$.

$$\delta_{\max}(mm) = 7.1496 \times 10^{-34} \frac{L_{(mm)}^{6.5} P_{(MPa)}^{1.993} T_{surf\,(^oC)}^{8.766}}{d_{(mm)}^{5.333}} \tag{5}$$

where P: ferrostatic pressure, L: roll pitch, T_{surf}: strand surface temperature, and d: solidified shell thickness.

Dynamic Bulging Model for Unsteady Bulging

Bulging of the strand involves both static and dynamic components according to time variations of the bulging which accompany the movement of the strand. Figure 1 illustrates steady and unsteady bulging. With steady bulging, the surface profile of strand is constant with time, and each portion of the steel shell follows the bulged profile, wiggling like a snake as it moves down with the casting speed. Although the strand bulges outwards between rolls and is pushed back beneath rolls, the mold level stays constant because the volume of molten steel obtained inside the solidifying shell does not change with time. In contrast, with unsteady bulging, the contorted shape of the strand surface becomes partially frozen, so the bulged profile moves down the caster. When the steady bulged shape of the solidified shell, called the "concave profile", moves between the rolls, the strand must be squeezed inwards. The total volume of molten steel contained within the strand decreases which causes the mold

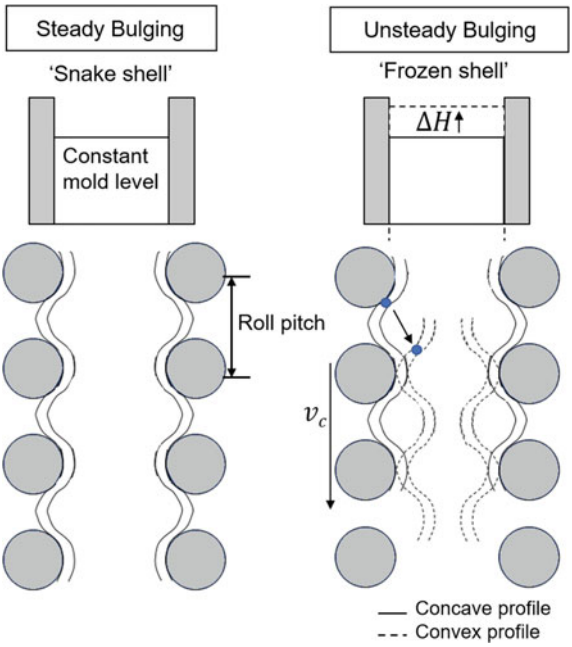

Fig. 1 Schematic illustration of steady, unsteady dynamic bulging

level to rise. Continuing down the caster, the strand experiences repeated transverse expansions and contractions, resulting in repeated vertical mold level fluctuations.

To model this behavior, molten steel flow is divided into three components: inflow into the mold through the stopper rod, outflow due to downward movement of the solidifying shell at the casting speed, and liquid steel flow due to transverse movement of the solidified shell. The latter component is found by tracking changes in the volume of the molten steel inside the solidified shell according to the shape of the bulged strand, the extent to which it is partially "frozen", and its downward movement. This volume change, ΔV_b, will induce mold level fluctuations, which the mold level control system will attempt to compensate. The resulting movement of the stopper rod, which changes the inlet steel flow from the tundish induces transient volume changes, ΔV_s. Any time variation in casting speed will introduce further volume changes, ΔV_o. As shown in Fig. 2, ignoring other effects, the following volume conservation equation gives the total time-varying volume change of the strand, ΔV_m:

$$\Delta V_m = -\Delta V_b + \Delta V_s - \Delta V_o \tag{6}$$

This total volume change of molten steel also can be found from the measured mold level fluctuations, ΔH:

$$\Delta V_m(t) = \Delta H(t) WD \tag{7}$$

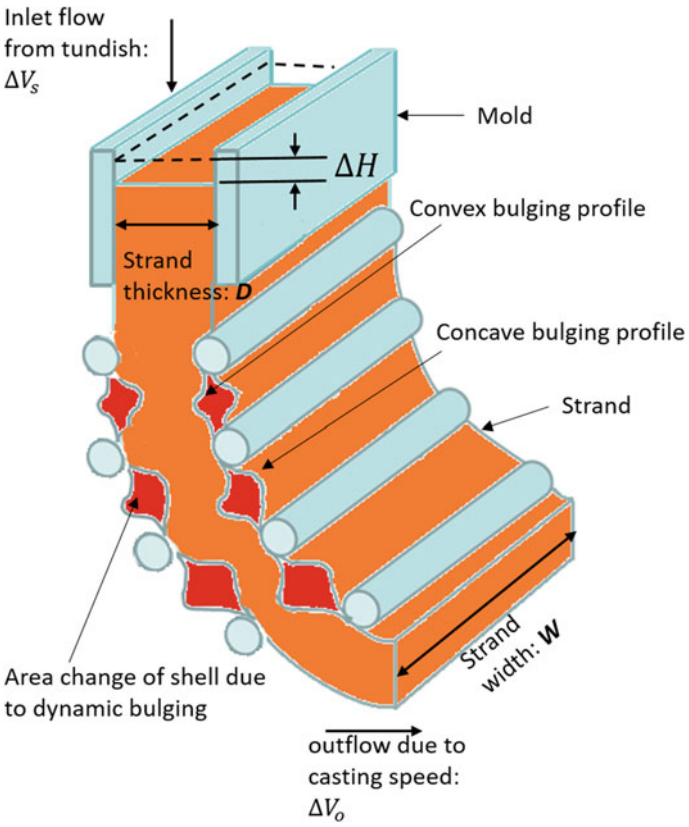

Fig. 2 Schematic diagram of evaluation of volume change by unsteady bulging

where W is strand width, D is strand thickness, and average $\Delta H(t)$ is estimated by the mold level sensor. In the steady-state, or "snaking shell" case, the volume change induced by bulging is zero, i.e. $\Delta V_b = 0$. In the partially frozen shell case, it depends on both the inter-roll bulging profile along the entire strand, and how that shape changes as it moves down the caster. In a slab caster with relatively constant width, this simplifies to

$$\Delta V_b = \sum A_i W \tag{8}$$

where A_i is area change in ith roll pitch induced by repeated transverse expansions and contractions of the strand.

The dynamic bulging model in this section is developed for the unsteady bulging case. For simplicity, the maximum bulging location is assumed to be at the center of the roll pitch, midway between rolls, and the bulging profile was very roughly approximated as triangular. Figure 3 shows the two extreme cases in unsteady bulging

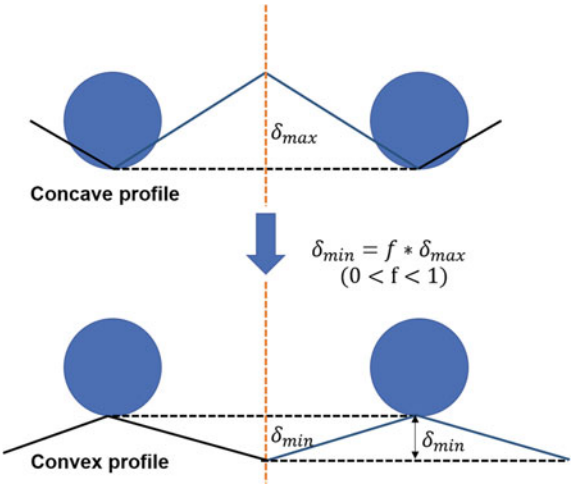

Fig. 3 Concave and convex profile of triangular bulging profile

over one roll pitch: concave and convex profiles. Due to creep deformation, the bulging amplitude is assumed to decrease after the bulged 'peak' moves from midway between rolls to lie directly under the next roll. The following assumptions were made for simplicity: (A1) this decrease in height happens linearly from concave profile to convex profile, and vice versa; (A2) $\delta_{\min} = f\delta_{\max}, f$ is set to be 0.5 in this study; (A3) The bulging at each roll pitch is independent.

To calculate the time evolution of the x–z area change of the bulging profile with strand movement, the concave profile of steady bulging was taken as the initial state. The passing line of steel strand was taken as the zero reference. Denoting z as the strand movement along the casting direction starting from time $t = 0$, the area change in a single roll pitch L can be calculated by

$$A_i(z) = \begin{cases} 0.5\left(\left(L-2z'\right)\left(1-\dfrac{2z'}{L}\right)-\dfrac{4z'^2}{L}\right)\left(1-(1-f)\dfrac{2z'}{L}\right)\delta_{\max}, \\ \quad z \in [nL, \dfrac{L}{2}+nL) \\ 0.5\left(-2\left(L-z'\right)*\left(1-\dfrac{2z'-L}{L}\right)+\dfrac{\left(2z'-L\right)^2}{L}\right)\left(f+(1-f)\dfrac{2z'-L}{L}\right)\delta_{\max}, \\ \quad z \in [\dfrac{L}{2}+nL, L+nL) \end{cases} \tag{9}$$

where $z' = z \mod L$, $n = 1, 2, \ldots\ldots$. The distance that the strand moved, $z(t)$, can be calculated from casting speed $v_c(t)$:

$$z(t) = \int_0^t v_c(\tau) d\tau \tag{10}$$

Based (A3), the total volume change due to bulging can be calculated by

$$\Delta V_b(t) = \sum A_i(z(t)) W \tag{11}$$

Stopper Rod Flow Model

A pressure drop—flow rate model for stopper rod systems (PFSR) is used to estimate the time-dependent inlet steel flow rate, based on the input stopper position history recorded at the plant. PFSR is a stand-alone MATLAB-based program that solves a system of Bernoulli equations for flow rate and pressure distribution down the entire system from tundish top surface, through SEN, to the mold top surface. Details of the model can be found in [17].

During continuous casting, the stopper rod is susceptible to erosion. To minimizing the effect of erosion, data were collected from temporal regions in the plant measurements where there was constant casting speed followed by a sudden change (increase or decrease of casting speed), and finally followed by another time period of constant casting speed. Throughput differences within this short period should be explained by the stopper rod movement.

The average erosion rate was estimated for the entire casting sequence, according to flow rate changes during times of constant speed. After accounting for the erosion, the stopper rod data were extrapolated to zero flow rate at zero stopper position. After further calibration and validation of PFSR with 18 sets of measurements, the following linear interpolation of the stopper rod inlet flow rate by PFSR was obtained.

$$Q_s(t) = 0.5924 * h(t) + 0.764 \tag{12}$$

where Q_s(ton/min) is the inlet flow through stopper rod opening and $h(t)$(mm) is a stopper rod opening. This linear interpolation is believed only valid for a narrow range of stopper rod (3.2–4.7 mm) and flow rate [2.66–3.53 (ton/min)], which happens to be relevant for typical casting conditions at the plant.

Computational Procedure

The calculation procedure of these models is as follows:

- ConOffline calculates the maximum bulging amplitude at each roll pitch based on recorded or specified casting conditions including slab geometry, casting speed,

spray flow rates, steel grade, etc., for each time step, Δt(1 s in this study), based on the shell thickness and surface temperature profiles down the strand from Eqs. (1–5).

- Next, the dynamic bulging model calculates the mold level fluctuation caused by volume changed due to bulging, $\Delta V_b(t)$ from Eqs. (6–12) knowing the local strand surface temperature, shell thickness, roll pitch, ferrostatic pressure, and casting speed.
- Inflow volume induced by stopper rod movements are calculated from the inlet steel flow based on Eq. (13), knowing the stopper rod position measurement $h(t)$ as follows:

$$\Delta V_s(t) = Q_s(t)\Delta t \tag{13}$$

- Outflow volume due to downward movement at the casting speed, $v_c(t)$, are found from:

$$\Delta V_o(t) = v_c(t)WD\rho\Delta t \tag{14}$$

  Since the casting speed is relatively constant during this simulation, the variation of $\Delta V_o(t)$ is almost negligible.
- The total volume change history in the mold can be calculated from Eq. (7) knowing the mold level position measurement.

Simulation Results and Discussion

Casting Conditions

The casting scenario simulated is shown in Fig. 4. The first plot shows the casting speed history, which is relatively constant around 3.1 m/min. The spray flow rate in secondary cooling zones 5 and 6 were increased at around 1000 s because large bulging in these 2 zones was suspected. The last two plots are measured mold level position and stopper rod position, which show evidence of significant dynamic bulging followed by a time interval where only small bulging is suspected. Steel composition was changed at around 2700 s, which appears to be at least partly responsible.

Stopper Rod Flow Model Results

First, the new volume model was applied to the measured scenario, including only the effect of stopper rod movements, and neglecting any dynamic bulging. A comparison

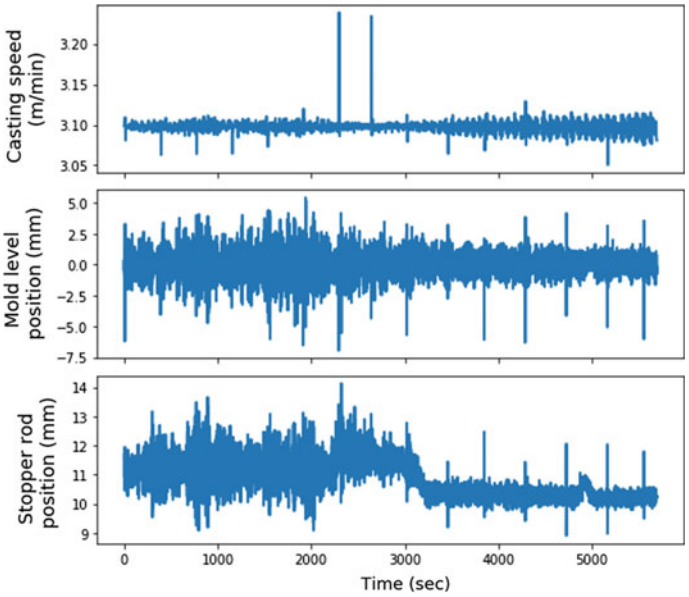

Fig. 4 Simulated casting scenario

of the calculated and measured mold level position histories are shown in Fig. 5 for two time intervals: 500–510 s (dynamic bulging suspected) and 3400–3410 s (no bulging problems suspected). Differences between the calculated mold level from the stopper rod flow model and the measured mold level should be explained by dynamic bulging. When dynamic bulging is suspected to be large (left figures), the model greatly over predicts the level fluctuations. This indicates that in the real caster, the level control system was compensating for those changes. This is also indicated by the difference between measured throughput, which was constant, and the model predicted inlet flow, which appears to have been almost exactly compensating for the significant dynamic bulging. When dynamic bulging was small, (right figures), the predicted mold level is similar to the measurements indicating that the mild level fluctuations are caused by stopper rod movement and surface waves.

To better illustrate the importance of dynamic bulging, the model prediction of the mold level (considering stopper rod movement only) was subtracted from the measured mold level signal, i.e. $\Delta V_m - \Delta V_s + \Delta V_o$, and converted into $\Delta H(t)$ using Eq. (7). This new prediction, "model prediction with no level control", represents the expected mold level history if the stopper opening had been held constant (i.e., with no level control system). This prediction is shown in Fig. 6 for the 500–520 s time interval, where it reveals much larger level fluctuations than the actual measured mold level. This confirms the suspicion that dynamic bulging must have been very severe during this time interval. Furthermore, it shows that the stopper rod movement due to the level control system was helping to decrease the mold level fluctuations. Note,

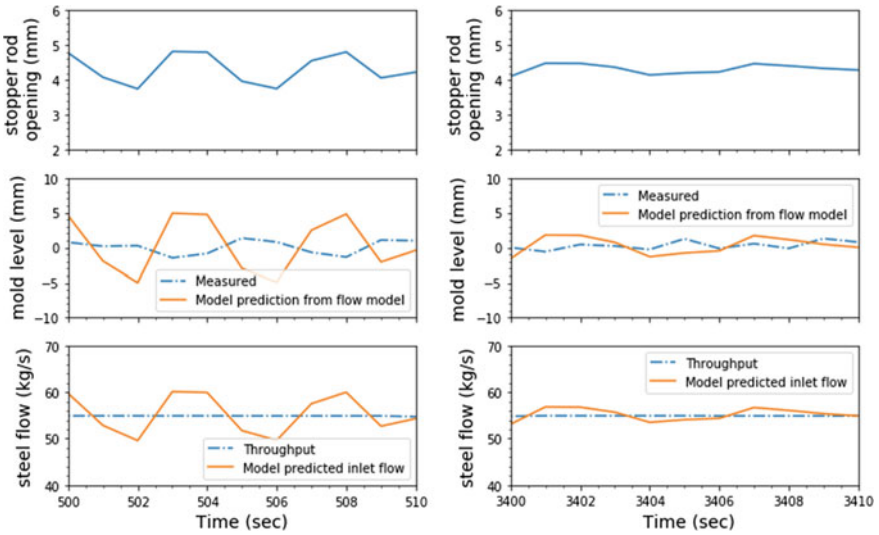

Fig. 5 Measured mold level position and calculated mold level position due to the variation of inlet steel flow

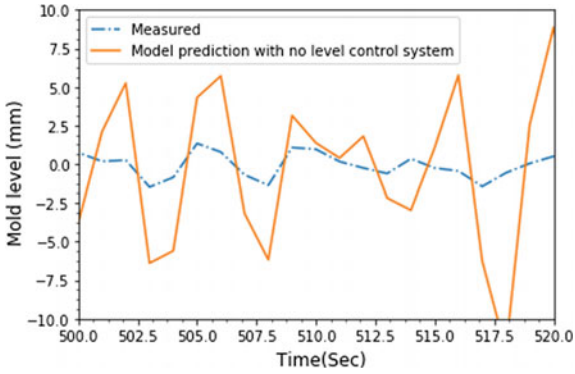

Fig. 6 Comparison of measured and calculated mold level histories, including dynamic bulging

however, that there is still much room for improvement, if the unsteady bulging could be decreased or eliminated, or the mold level control system could be improved.

Dynamic Bulging Model Results

Next, to predict dynamic bulging, the bulging amplitude calculated from Eq. (5) was simulated for each roll pitch, and used to predict the mold level fluctuation induced by dynamic bugling. The "model prediction with no level control" explained in the Section "Stopper Rod Flow Model Results", which is the differences between

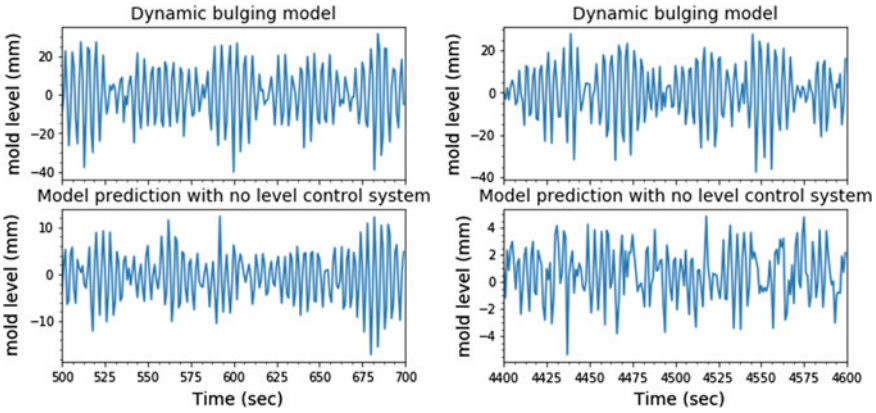

Fig. 7 Mold level prediction with dynamic bugling model and mold level prediction with no control system for 500–700 s and 4400–4600 s

the calculated mold level from the stopper rod flow model and the measured mold level, was used as a comparison to the dynamic bulging model prediction. Figure 7 shows this two predictions for time intervals of 500–700 s and 4400–4600 s. In the case of 500–700 s, significant dynamic bulging was suspected, the magnitude of the prediction from the dynamic bulging model is two times bigger than the model prediction with no level control system. We argue that this difference is caused by assuming dynamic bugling in all zones in the dynamic bulging model, while in the real caster, it may be steady bulging in certain regions and dynamic unsteady bulging in other regions. The trend of the two signals shows a qualitative match with similar clustering of the peaks. However, for 4400–4600 s, the two signals do not match. This suggests that after the steel grade change, the new shell becomes more susceptible to creep, so the bulging profile reverts from dynamic to more steady bulging, with smaller f-value, and thus reduces the volume changes and mold level fluctuations. Indeed, with minimal dynamic bulging, the measured signal is more likely to be caused by random turbulent flow and surface waves, which cannot be controlled by stopper rod movement.

Power spectrum density (PSD) analysis of the signals in Fig. 7 is shown in Fig. 8. The period used for Fast Fourier Transform is 200 s. When bad dynamic bulging is suspected (500–700 s), the PSD of the measured signal shows that the main frequency is the frequency corresponding to the roll pitch in zone 5, while the PSD of the estimation shows matching frequency at zone 5, and zone 6. When small dynamic bulging is suspected (4400–4600 s), the PSD of the measurement shows no matching frequency of roll pitch in spray zones, and it appears to be random noise. This also supports the hypothesis that there is steady bulging for 4400–4600 s. The PSD of the estimation still shows the main frequency of the roll pitch of zone 5, and 6 but

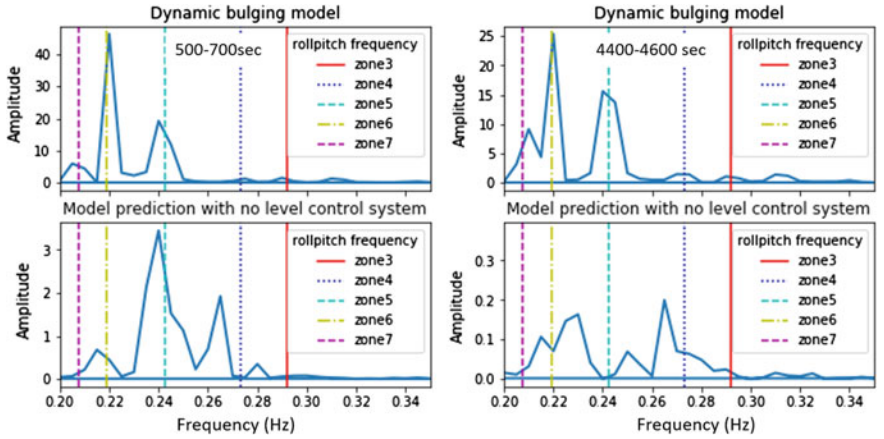

Fig. 8 Power spectrum analysis of the measured and estimated mold level position-time signals shown in Fig. 7

with smaller magnitude. This is because the dynamic bulging model was simulating a case of unsteady bulging throughout the caster. Therefore, it should not match the steady bulging results.

Conclusions

A dynamic volume model has been developed to relate the volume changes from dynamic unsteady bulging and stopper rod movements to level fluctuations in the continuous slab-casting process. The model incorporates separate submodels to predict steady-state bulging and the relation between flow rate and pressure drops according to stopper rod position. Model predictions of the history of mold level variations caused by unsteady bulging matches reasonably with measurements of mold level history in a thin-slab caster. Power Spectrum Density analysis shows that for the studied case, dynamic bulging in zone 5 appears to be responsible for the level fluctuations, as the dynamic volume model is able to catch the zone 5 frequency peaks. This work confirms that dynamic bulging is responsible for significant mold level fluctuations in the plant under some circumstances. Furthermore, the model shows that the mold level control system only partly compensates for the dynamic bulging, making mold level fluctuation only slightly less severe than would have occurred with a constant stopper position. This leaves a lot of room for future improvement of mold level control systems. This work is only a preliminary first step to model unsteady dynamic bulging. To fully understand dynamic bulging, much further work is needed.

Acknowledgements This work was supported by NSF Grant #1300907, NSF INTERN DCL #1747876, and the Continuous Casting Center at the Colorado School of Mines. Special thanks are extended to Nucor Steel Decatur for providing caster data and casting conditions.

References

1. Dalin J, Chenot J (1988) Finite element computation of bulging in continuously cast steel with a viscoplastic model. Int J Numer Methods Eng 25(1):147–163
2. Barber B, Lewis BA, Leckenby BM (1985) Finite-element analysis of strand deformation and strain distribution in solidifying shell during continuous slab casting. Ironmak Steelmak 12(4):171–175
3. Ohno H, Miki Y, Nishizawa Y (2016) Generation mechanism of unsteady bulging in continuous casting-1-Development of method for measurement of unsteady bulging in continuous casting. ISIJ Int 56(10):1758–1763
4. Yoon U-S, Bang I-W, Rhee JH, Kim S-Y, Lee J-D, Oh KH (2002) Analysis of mold level hunching by unsteady bulging during thin slab casting. ISIJ Int 42(10):1103–1111
5. Manayathara TJ, Tsao T-C, Bentsman J (1996) Rejection of unknown periodic load disturbances in continuous steel casting process using learning repetitive control approach. IEEE Trans Control Syst Technol 4(3):259–265
6. Dussud M, Galichet S, Foulloy LP (1998) Application of fuzzy logic control for continuous casting mold level control. IEEE Trans Control Syst Technol 6(2):246–256
7. Lee JD, Yim CH (2000) The mechanism of unsteady bulging and its analysis with the finite element method for continuously cast steel. ISIJ Int 40(8):765–770
8. Yu L (2000) FEM analysis of bulging between rolls in continuous casting. M.S. thesis, University of Illinois Urbana-Champaign
9. Miyazawa K, Schwerdtfeger K (1979) Computation of bulging of continous of bulging in continuously cast slabs wiht simple bending theory. Ironmak Steelmak 6(2):68–74
10. Petrus B, Zheng K, Zhou X, Thomas BG, Bentsman J (2011) Real-time, model-based spray-cooling control system for steel continuous casting. Metall Mater Trans B 42(1):87–103
11. Chen Z, Bentsman J, Thomas BG, Matsui A (2017) Study of spray cooling control to maintain metallurgical length during speed drop in steel continuous casting. Iron Steel Technol 14(10):92–103
12. Petrus B, Chen Z, Bentsman J, Thomas BG (2018) Online recalibration of the state estimators for a system with moving boundaries using sparse discrete-in-time temperature measurements. IEEE Trans Automat Contr 63(4):1090–1096. https://doi.org/10.1109/TAC.2017.2736950
13. Chen Z, Bentsman J, Thomas BG (2018) Bang-Bang free boundary control of a Stefan problem for metallurgical length maintenance. Paper presented at the Am Control Conf., Milwaukee, 27–29 June 2018. https://doi.org/10.23919/acc.2018.8431904
14. Petrus B, Hammon D, Miller M, Williams B, Zewe A, Chen Z, Bentsman J, Thomas BG (2015) New method to measure metallurgical length and application to improve computational models. Iron Steel Technol 12(12):58–66
15. Duvvuri P, Petrus B, Thomas BG (2014) Correlation for mold heat flux measured in a thin slab casting mold. Paper presented at the AISTech—Iron and steel technology conference, Indianapolis, 5–8 May 2014
16. Nozaki T, Matsuno J, Murata K, Ooi H, Kodama M (1978) A secondary cooling pattern for preventing surface cracks of continuous casting slab. Trans. Iron Steel Inst Jpn 18(6):330–338
17. Olia H, Thomas BG (2018) Flow rate—stopper position model of NUCOR caster using Pressure Drop Flow Rate Model for Stopper Rod Flow Control Systems (PFSR). Report presented at CCC annual meeting, Golden